Chinese Chemical Letters 33 (2022) 773–777

Contents lists available at ScienceDirect

Chinese Chemical Letters

journal homepage: www.elsevier.com/locate/cclet

Target-triggered hairpin-free chain-branching growth of DNA dendrimers for contrast-enhanced imaging in living cells by avoiding signal dispersion

Jiaqi Deng[a,1], Jingyuan Xu[a,1], Minzhi Ouyang[c,1], Zhen Zou[a], Yanli Lei[a], Junbin Li[a], Zhihe Qing[a,*], Ronghua Yang[b,*]

[a] Hunan Provincial Key Laboratory of Cytochemistry, School of Chemistry and Food Engineering, Changsha University of Science and Technology, Changsha 410114, China
[b] Laboratory of Chemical Biology & Traditional Chinese Medicine Research, Ministry of Education, College of Chemistry and Chemical Engineering, Hunan Normal University, Changsha 410081, China
[c] Department Ultrasound Diagnosis, The Second Xiangya Hospital, Central South University, Changsha 410011, China

ARTICLE INFO

Article history:
Received 11 May 2021
Revised 7 August 2021
Accepted 8 August 2021
Available online 12 August 2021

Keywords:
Cell imaging
Amplification
Signal dispersion
Self-assembly
DNA dendrimers

ABSTRACT

The development of amplification strategies is one of the central challenges for detection of low-abundance targets. One-to-many (1:M) amplification strategies in which one target lights many signal probes, has improved the detection sensitivity in bulk solution, but with discounted contrast in cell imaging, because the lighted probes are dissociative and dispersible. In this work, a one-to-large (1:L) signaling mechanism, in which the lighted probes were orderly connected to each other, was conceptually proposed to enhance the contrast in cell imaging by avoiding signal dispersion in amplification. Accordingly, target-triggered hairpin-free chain-branching assembly (HFCBA) holds great potential to implement the 1:L mechanism, but using it in cell imaging has yet to be demonstrated. As a proof of concept, a group of probes were first programmed to implement miRNA-21-triggered HFCBA. After transfection of probes, gradually-growing signal flares in cells were monitored along with the growth of DNA dendrimers; and the *in situ* fluorescence accumulation in HFCBA resulted in highly-enhanced contrast to the surrounding by avoiding signal dispersion in amplification. The contrast-enhanced imaging with signal amplification is significant for biological analysis and molecular medicine. We expect the 1:L mechanism will provide a new thought for high-performance imaging of biomarkers in cells.

Cells comprise a large variety of bio-molecules, whose configurations and concentrations are always precisely controlled in a healthy state, but the variation in the expression level of a certain functional bio-molecule is generally related to diseases [1,2]. For example, over-expression of small microRNA (miRNA) is found to associate with the growth and progression of cancer [3–5]. Thus, the development of selective technologies to report the behaviors of intracellular molecules of interest is significant for biology and medicine. By virtue of its relatively high-resolution, non-radiation and safe-detection, fluorescent imaging has been greatly promoted and used for the acquisition of intracellular biochemical information [6–11].

Design of fluorescent probes for cell imaging has primarily relied on the one-to-one (1:1) signaling mechanism, in which one target binds with one probe, resulting in one signal (Scheme 1, a1) [12–16]. One-to-one imaging strategy can respond to targets at high concentrations and produce an elevated signal with reference to the surrounding, but it is not able to monitor fluctuation of target amount at low-abundance levels [17,18]. Thus, amplification-based imaging strategies are required to solve the challenge, and the one-to-many (1:M) signaling mechanism has been developed, in which one target triggers a cascade of reactions between probes, resulting in many signals (Scheme 1, a2) [17,19]. Especially with the advance of isothermal amplification techniques in the past years, various strategies have been even reported for 1:M imaging of biomarkers in living cells, not only for sensitive detection in fixed cells or cell lysate, based on dynamic DNA self-assembly [20–22], fuel stimulants [23,24], and DNAzyme motors [25–27]. Undoubtedly, the 1:M mechanism can really improve the signaling

* Corresponding authors.
E-mail addresses: qingzhihe@hnu.edu.cn (Z. Qing), Yangrh@pku.edu.cn (R. Yang).
[1] These authors contributed equally to this work.

https://doi.org/10.1016/j.cclet.2021.08.046
1001-8417/

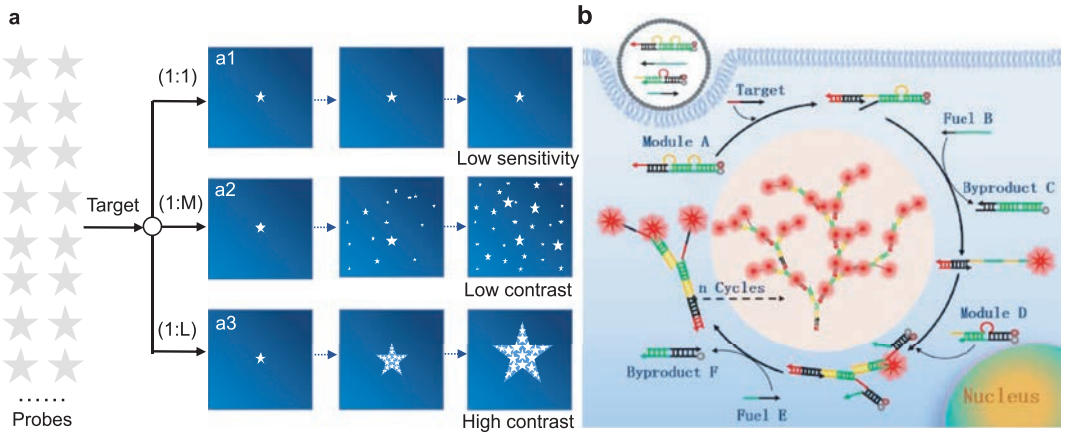

Scheme 1. (a) Schematic illustration of different signaling strategies. a1, one-to-one (1:1) signaling mechanism with low sensitivity; a2, one-to-many (1:M) strategy with signal amplification but low contrast in imaging; a3, one-to-large (1:L) strategy with signal amplification and high contrast in imaging. (b) Schematic illustration of target-triggered growth of DNA dendrimers as a 1:L strategy for contrast-enhanced imaging of miRNA in living cells, by avoiding signal dispersion in amplification.

sensitivity towards the target at low concentration in bulk solution. However, one can see that the lighted probes in 1:M signaling model are generally dissociative and can easily diffuse apart, resulting in signal dispersion and discounted contrast in imaging [18,21,22,24,25,28], which is impeditive for high-resolution and *in situ* analysis [29–31]. Here, a one-to-large (1:L) signaling mechanism is proposed to enhance the contrast in cell imaging. In 1:L amplification, one target is designed to trigger a cascade of reactions between probes, the lighted probes connect orderly to each other, forming a larger and larger nanostructures with bright fluorescence. The larger structure holds lower mobility, and the fluorescence accumulation from connected probes displays enhanced-contrast to the surrounding (Scheme 1, a3).

In comparison to hairpin DNA-based dynamic self-assembly (*e.g.*, hybridization chain reaction), hairpin-free chain-branching assembly (HFCBA) increases the stability of the assembled products and allows very flexible sequence design [32–34]. In addition, HFCBA holds great potential to meet the criterion of 1:L signaling mechanism, but using it in cell imaging has yet to be demonstrated. In this work, to establish a prototype of the 1:L signaling mechanism for contrast-enhanced imaging by avoiding signal dispersion, miRNA-21, which is an intracellular biomarker of malignant tumors [26], is selected as the model target; a group of metastable DNA probes including two double-stranded modules (A and D) and two single-stranded fuels (B and E) are first programmed to implement HFCBA in living cells (Scheme 1b). The modules and fuels are co-delivered into cytoplasm by using the highly efficient transfection approach. The target T hybridizes to the exposed toehold of module A and initiates a cascade of strand displacement reactions. As a result, the BHQ2-modified strands of modules A and D are eliminated to form byproducts C and F, with the assistance of fuels B and E. The TAMRA-modified strands of modules A and D assemble together to form DNA dendrimers with lighting of fluorescence. With the process of target-triggered strand displacement reactions, the DNA dendrimer grows gradually. In this way, many lighted fluorophores are connected to the target root, with signal accumulation at one site. Thus, via target-triggered growth of fluorescent DNA dendrimers in living cells, contrast-enhanced imaging should be realized in this 1:L mechanism by avoiding signal dispersion in amplification.

Target-triggered growth of DNA dendrimers by HFCBA was first characterized. Modules A and D were prepared respectively by annealing the mixture of the TAMRA-labeled strand (10 μmol/L) and the BHQ2-labeled strand (10 μmol/L), which was heated to 95 °C for 5 min and cooled slowly to room temperature. From polyacrylamide gel electrophoresis (Fig. 1a), with the sequential introduction of modules (A and D) and fuels (B and E), one can see that the modules gradually assembled to larger complexes with slower electrophoresis motion, and that the fuels displaced the BHQ2-labeled strands of modules to form by-products (C and F). The response of fluorescence signal to the target was also measured (Fig. 1b). In the absence of the target, the detection system displayed very low fluorescence signal after incubation for 4 h (black curve); while the system with 20 nmol/L target displays strong fluorescence emission of TAMRA after growth of DNA dendrimers (red curve), indicating successful HFCBA triggered by the target. In addition, only in the presence of all designed modules and fuels, the HFCBA amplification system could work well, much weaker fluorescence response would be detected for the target if there was a lack of any unit (Figs. S1 and S2 in Supporting information). Thus, these results demonstrated a good feasibility for target-triggered growth of DNA dendrimers as our design. To further visually con-

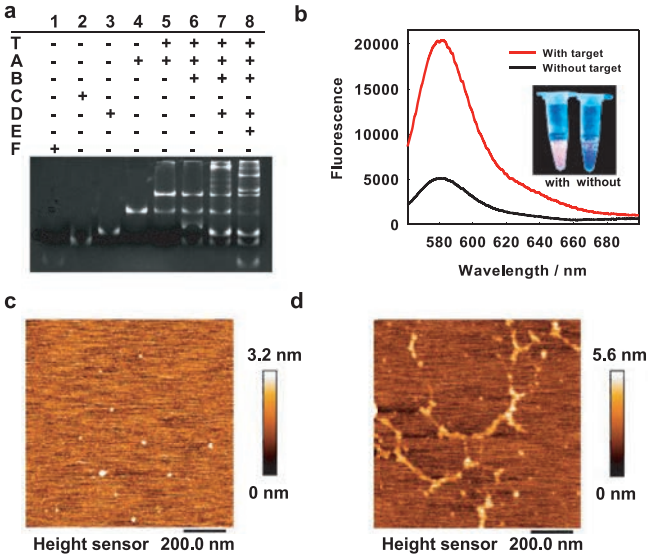

Fig. 1. Feasibility verification of target-triggered growth of DNA dendrimers. (a) Electrophoresis characterization of target-triggered growth of DNA dendrimers, as a step-by-step procedure. (b) Fluorescence spectra of the system in the absence (black curve) or presence of the target (red curve). The excitation wavelength of TAMRA was set at 542 nm, and its maximum emission at 582 nm was measured. The insert was the corresponding image under UV irradiation. AFM imaging of HFCBA products in the absence of the target (c) and in the presence of the target (d).

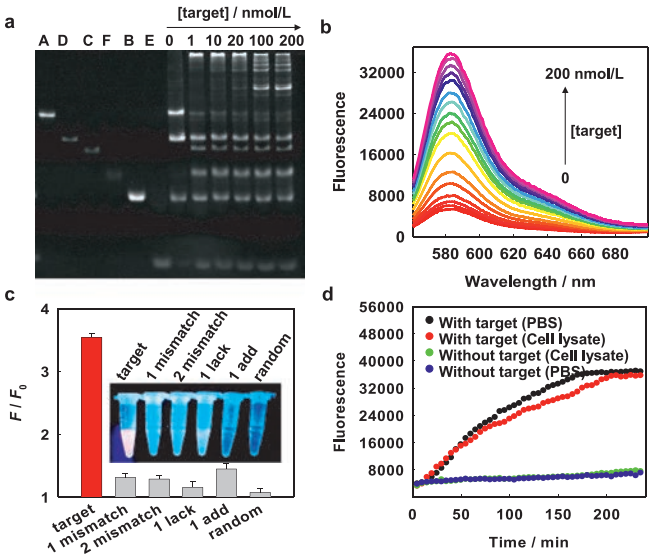

Fig. 2. Target detection in bulk solution by the proposed strategy for the target. (a) Electrophoresis characterization of growth products induced by the target of different concentrations. (b) Fluorescence spectra as the increase of the target concentration. (c) Signal-to-background (F/F_0) towards different targets. The insert was the corresponding image under UV irradiation, the detected concentration of each DNA was 20 nmol/L. (d) Real-time monitoring of fluorescence responses in PBS buffer and the complex biological fluid (red blood cell lysate).

firm target-triggered growth of DNA dendrimers, the assembled complexes were imaged by atomic force microscope (AFM). In the absence of the target, only tiny spots were shown in the AFM image (Fig. 1c). In contrast, after incubation with the target, large branched structures were observed (Fig. 1d), which was visual evidence that the target-triggered growth of DNA dendrimers indeed took place as expected, and in consistent with the above results.

Then, effects of some important conditions on target-triggered growth of fluorescent DNA dendrimers were investigated to get better performance before application of this signaling mechanism for target detection *in vitro* and in cells. As show in Fig. S3 (Supporting information), with the increase of assembly time until 4 h, the bands A and D in electrophoresis became weaker and weaker, the bands C and F became brighter and brighter, indicating the gradual consumption of models and generation of by-products along with the target-triggered growth of fluorescent DNA dendrimers. Subsequently, assembly temperature, module concentration and the ratio of module to fuel were optimized by the manner of signal-to-background ratio (F/F_0), where F_0 was the fluorescence intensity of the detection system in the absence of the target, and F was that in the presence of the target. One can see that there was relatively-good detection performance under both room temperature (25 °C) and physiological temperature (37 °C) (Fig. S4 in Supporting information). 100 nmol/L model A was optimal when a relatively-low target concentration (20 nmol/L) was used and the ratio of model A to D was set at 1:2 (Fig. S5 in Supporting information). The increase of fuel strands amount could obviously improve the signal-to-background ratio, and a ratio (module to fuel) of 1:3 was selected for further detection system (Fig. S6 in Supporting information).

Subsequently, the capability of the proposed 1:L mechanism to detect the target miRNA-21 was investigated. As shown in the gel electrophoresis (Fig. 2a), when in the absence of the target, only the bands of modules (A and D) and fuels (B and E) were imaged in the gel. However, when a low-concentration target (1 nmol/L) was introduced into the 1:L detection system, a bright band indicating a lager assembly product appeared in the injection port, accompanied with the generation of by-products (C and F). Along with the increase of the target concentration, other bands indicating products of different weight were observed, which was due to the fact that more targets induced more DNA dendrimers, but the amount of substrates was fixed, thus resulting in smaller dendrimers. The response of fluorescence signal to the target of different concentrations was also measured. Fluorescence emission intensity of TAMRA at 582 nm climbed up gradually with the increase of target concentration (Fig. 2b). The relationship between the fluorescence intensity and the target concentration was shown in Fig. S7 (Supporting information), there was a linear range from 10 pmol/L to 20 nmol/L, $R^2 = 0.9918$, the detection limit (LOD) was calculated to be 0.66 nmol/L based on the three times of the standard deviation of the blank signal (3σ). The selectivity towards the target was investigated by detecting different sequences, including base mismatching, lacking, adding and random sequence. From Fig. S8 (Supporting information) and Fig. 2c, there was little interference from control sequences and a good selectivity was demonstrated for target detection.

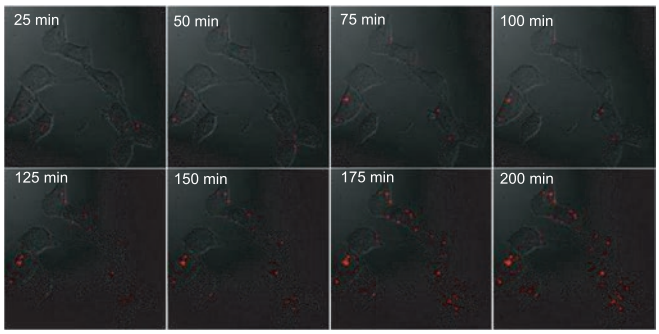

Fig. 3. Real-time imaging of miRNA-21 in MCF-7 cancer cells after incubation with probes-loaded liposome for different time.

Before exploring the ability of the 1:L signaling mechanism for contrast-enhanced imaging of miRNA-21 in living cells, the nuclease resistance of DNA moieties and target-triggered DNA dendrimers was first investigated. As shown in Fig. S9 (Supporting information), all DNA moieties and DNA dendrimers displayed good nuclease resistance when treatment with 0.5 U/mL DNase I, this was due to the incorporation of locked nucleic acid (LNA) nucleotides in each DNA. Then, the response to the target in the complex biological fluid was investigated. The red blood cell lysate was used as a complex biological fluid. The fluorescence intensity at 582 nm with adding the target into the lysate was much higher than that in the absence of the target, and the time-dependent fluorescence responses to the introduction of the target in both cell lysate and PBS buffer were almost the same (Fig. 2d), indicating that the target-triggered HFCBA growth of fluorescent DNA dendrimers could be applied for target detection in the complex biological fluid. After that, the cytotoxicity of the 1:L system was investigated, high viability of MCF-7 and L0–2 cells after incubation for different time (12, 24, 36 h) proved a good biocompatibility of the 1:L system (Fig. S10 in Supporting information).

Subsequently, the proposed amplification mechanism was applied for *in situ* imaging of miRNA-21 in living cells. The mixture of modules and fuels was transfected into cell by liposome 3000. Co-localization experiments with tracking dyes showed that the fluorescent DNA dendrimers located in the cytoplasm (Fig. S11 in Supporting information). Along with incubation of probes-loaded liposome, real-time fluorescence imaging was carried out for MCF-7 cancer cells, in which miRNA-21 is over expressed. As shown in Fig. 3, one can see that the fluorescence signal in images was present as point-like distribution, and the size of signal flares became larger and larger with the increase of incubation time, indicating the target-triggered gradual growth of fluorescent DNA

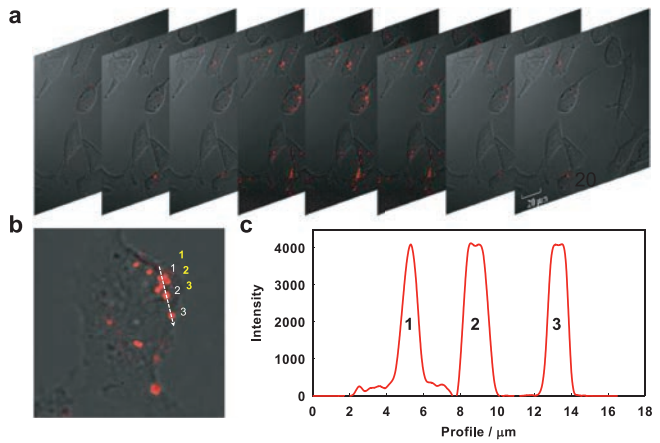

Fig. 4. (a) The z-stack images of MCF-7 cells after miRNA-21-triggered HFCBA for 4 h. (b) An enlarged image of MCF-7 cells after miRNA-21-triggered HFCBA. (c) The fluorescence intensity corresponding to the dotted lines in (b).

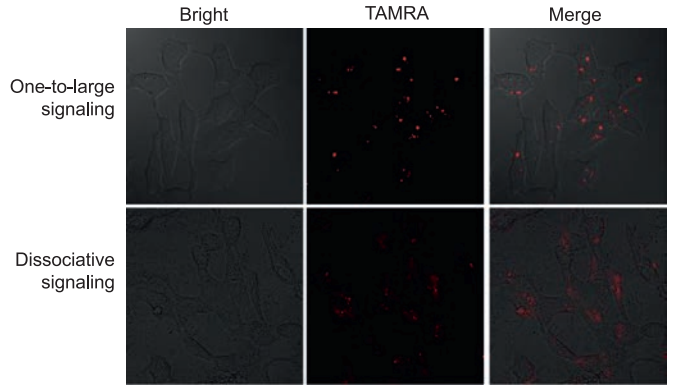

Fig. 5. Comparison of tow imaging manners including one-to-large signaling (up) and dissociative signaling (down). The one-to-large signaling was *in situ* implemented in living cells *via* miRNA-21-triggered HFCBA. The dissociative signaling as a control was executed by transfecting the annealing product of the target and its molecular beacon at a 1:1 ratio. The concentration of the molecular beacon was equal to the sum of modules (A and D), whose fluorophore TAMRA was at a low total concentration of 12.6 nmol/L in transfection.

dendrimers in living cells. By virtue of the one-to-large signaling mechanism, the signal flares had clear boundaries to the surrounding; negligible signal dispersion was observed along with the signal growth. Thus, contrast-enhanced cell imaging was achieved in amplification. To visualize the cellular localization of the signal flares, z-stack imaging of MCF-7 cells after incubation with the 1:L system for 4 h was performed (Fig. 4a). As the movement of the confocal plane, the fluorescence signal changed to be stronger and then weaker, indicating the intracellular localization of the signal flares. The discrete distribution of fluorescence intensity in cells further verified the one-to-large amplification mechanism with high contrast (Figs. 4b and c).

Finally, the proposed 1:L signal mechanism was applied to visualize target miRNA-21 in different cells. A cancer cell line (MCF-7) and a control normal cell line (L0-2) were used. Same amount of models and fuels were transfected into cells and incubated in 37 °C incubator for 4 h, and then fluorescence imaging was carried out. Even if the total concentration of fluorophore TAMRA was low to 12.6 nmol/L in transfection, independent fluorescence flares that were highly contrast-enhanced to the surrounding were observed in MCF-7 cells, due to high-expression of miRNA-21 in them (Fig. 5, up); while no fluorescence signal was recorded in normal L0-2 cells (Fig. S12 in Supporting information). As a comparison, a group of dissociative probes was also transfected into cells, obvious signal dispersion and low contrast were observed from the dissociative signaling (Fig. 5, down). The *in situ* detection capability for miRNA-21 in living cells was also verified by flow cytometry. Compared with the blank, high statistical signal was obtained towards cancer cells, while negligible signal towards L0-2 cells (Fig. S13 in Supporting information), which were consistent with the results from confocal imaging. Therefore, the proposed 1:L signal mechanism based on target-triggered HFCBA growth of fluorescent DNA dendrimers has been successfully exploited for target detection in living cells, with contrast-enhanced imaging.

In summary, a one-to-large (1:L) signaling mechanism, in which one target can not only light a series of probes and the lighted probes also connect to each other through the HFCBA strategy to form larger and larger fluorescent DNA dendrimers, was proposed to enhance contrast in cell imaging by avoiding signal dispersion in amplification. To establish a prototype of this mechanism, a strategy based on hairpin-free chain-branching assembly was developed to detect the cancer biomarker miRNA-21. A group of probes to execute this strategy were designed and their sequences were reasonably programmed. Results verified there was a good performance including sensitivity and selectivity for the target detection in both buffer and biological fluid. Especially, *in situ* growth of signal flares was monitored in cancer cells and highly-enhanced contrast to the surrounding was imaged, which is importantly significant for life analysis and molecular medicine.

Declaration of competing interest

None of the authors have any financial affiliations that may be perceived to have biased the presentation.

Acknowledgments

This work was supported in part by the financial support through the National Natural Science Foundation of China (Nos. 22074008, 91853104, 32001782), and the Natural Science Foundation of Hunan Province (No. 2019JJ30025).

Supplementary materials

Supplementary material associated with this article can be found, in the online version, at doi:10.1016/j.cclet.2021.08.046.

References

[1] L. Gu, S.C. Frommel, C.C. Oakes, et al., Nat. Genet. 47 (2015) 22–30.
[2] D.J. Surmeier, J.A. Obeso, G.M. Halliday, Nat. Rev. Neurosci. 18 (2017) 101–113.
[3] J. Su, F. Wu, H. Xia, et al., Chem. Sci. 11 (2020) 80–86.
[4] S. Ali, A. Ahmad, S. Banerjee, et al., Cancer Res. 70 (2010) 3606–3617.
[5] K. Gumireddy, D.D. Young, X. Xiong, et al., Angew. Chem. Int. Ed. 47 (2008) 7482–7484.
[6] M. Bates, B. Huang, G.T. Dempsey, et al., Science 317 (2007) 1749–1753.
[7] H.Q. Chu, J. Zhao, Y.S. Mi, et al., Angew. Chem. Int. Ed. 58 (2019) 14877–14881.
[8] W. Zhang, J. Zhang, P. Li, et al., Chem. Sci. 10 (2019) 879–883.
[9] J. Zhao, H.Q. Chu, Y. Zhao, et al., J. Am. Chem. Soc. 141 (2019) 7056–7062.
[10] S. Griesbeck, E. Michail, C.G. Wang, et al., Chem. Sci. 10 (2019) 5405–5422.
[11] T. Ueno, T. Nagano, Nat. Methods 8 (2011) 642–645.
[12] T. Terai, T. Nagano, Curr. Opin. Chem. Biol. 12 (2008) 515–521.
[13] J. Zheng, R.H. Yang, M.L. Shi, et al., Chem. Soc. Rev. 44 (2015) 3036–3055.
[14] T.T. Meng, Y.X. Liu, M. Tan. Liu, et al., Chin. Chem. Lett. 26 (2015) 1179–1182.
[15] Y.B. Zhou, X.F. Zhang, S. Yang, et al., Anal. Chem. 89 (2017) 4587–4594.
[16] X. Wang, P. Li, Q. Ding, et al., Angew. Chem. Int. Ed. 58 (2019) 4674–4678.
[17] R.I. Wang, L. Lan, L. Liu, et al., Chin. Chem. Lett. 31 (2020) 159–162.
[18] Z.K. Wu, H.H. Fan, N.S.R. Satyavolu, et al., Angew. Chem. Int. Ed. 56 (2017) 8721–8725.
[19] Z.H. Qing, J.Y. Xu, J.L. Hu, et al., Angew. Chem. Int. Ed. 58 (2019) 11574–11585.
[20] P. Liu, X.H. Yang, Q. Wang, et al., Chin. Chem. Lett. 25 (2014) 1047–1051.
[21] C.C. Wu, S. Cansiz, L.Q. Zhang, et al., J. Am. Chem. Soc. 137 (2015) 4900–4903.
[22] H. Shi, T. Jin, J.W. Zhang, et al., Chin. Chem. Lett. 31 (2020) 175–178.
[23] X.W. He, T. Zeng, Z. Li, et al., Angew. Chem. Int. Ed. 55 (2016) 3073–3076.
[24] C.P. Liang, P.Q. Ma, H. Liu, et al., Angew. Chem. Int. Ed. 56 (2017) 9077–9081.
[25] Y.N. Wu, J. Huang, X.H. Yang, et al., Anal. Chem. 89 (2017) 8377–8383.
[26] P.J. Zhu, Y.Y. Zhang, S.X. Xu, et al., Chin. Chem. Lett. 30 (2019) 58–62.

[27] H. Wang, H.M. Wang, Q. Wu, et al., Chem. Sci. 10 (2019) 9597–9604.
[28] A.P.K.K.K. Mudiyanselage, Q. Yu, M.A. Leon-Duque, et al., J. Am. Chem. Soc. 140 (2018) 8739–8745.
[29] L.Y. Zhou, X.B. Zhang, Y.F. Lv, et al., Anal. Chem. 87 (2015) 5626–5631.
[30] H.W. Liu, K. Li, X.X. Hu, et al., Angew. Chem. Int. Ed. 56 (2017) 11788–11792.
[31] Z.H. Qing, J.L. Hu, J.Y. Xu, et al., Chem. Sci. 11 (2020) 1985–1990.
[32] F. Xuan, I.M. Hsing, J. Am. Chem. Soc. 136 (2014) 9810–9813.
[33] F. Xuan, T.W. Fan, I.M. Hsing, ACS Nano 9 (2015) 5027–5033.
[34] Q. Xue, C. Liu, X. Li, et al., Bioconjugate Chem. 29 (2018) 1399–1405.